MODELING STUDIES OF INK, PLATE AND FOUNTAIN INTERACTIONS BY CONTACT ANGLE MEASUREMENTS

Jianbing Huang* and Richard M. Goodman*

Keywords: Surface, Contact angle, Spreading index, lithography, Printing Plates.

Abstract: Spreading index has been considered as an important property for an ink-plate-fountain system. A new method is proposed to measure spreading index from the contact angles of fountain surrounded ink droplets and ink surrounded fountain droplets on plate image area. Application to model systems has illustrated the capability of the proposed method to probe three-phase interactions, for which a previous method is inherently deficient. With the proposed method, the adverse effect of surface active species in fountain solutions on spreading index in the plate image area is demonstrated. Also demonstrated is the difference between Soy oil and mineral oil.

SPREADING INDEX IN OFFSET PRINTING

In lithographic printing, uniform ink films formed by a train of ink rollers are patterned by a printing plate and then transferred directly or indirectly to paper or other substrates. The mechanism whereby a printing plate generates patterned ink films primarily involves a series of film splitting modes at the nips of plate cylinder and inker form rollers and, for conventional dampening system, at the nips of a plate cylinder and dampener rollers. MacPhee proposed two fundamental film splitting modes, 50/50 splitting and composite film splitting (MacPhee, 1979). In 50/50 splitting, liquid films before the center of a nip merge into a homogenized film, which then splits equally into two films carried away by two leaving surfaces at the nip. For composite film splitting, two liquid films before the center of a nip merge into a two layer composite film, which then splits in the less viscous layer usually consisting of fountain solutions. In normal printing, a 50/50 film splitting happens at the nips where inker form rollers meet plate image area, and, for conventional dampening system, at the nips where the dampener rollers meet plate non-image area. Composite film splitting occurs at the nips where inker form

* Polychrome Corporation, Carlstadt, New Jersey

rollers meet plate non-image area. If a given film-splitting mode occurs at a wrong place, a problem will be encountered. For example, if a composite film splitting mode occurs at the nip where an inker form roller meets plate image area, a printed stock may have missing images, a phenomenon commonly referred to as blinding. If a 50/50 film splitting occurs at a nip where an inker form roller meets a plate non-image area, a printed stock may show a dirty background, a phenomenon commonly referred to as scumming.

What mode of film splitting occurs at a given place is determined by what covers the plate when it enters into a nip. The latter has been addressed in literature by a model of competitive spreading (Bassemir, 1982). Based on this model, a spreading index is defined as the difference between the spreading coefficients of ink (S_i) and fountain solution (S_f) on plate surface.

$$\Delta S = S_i - S_f \tag{1}$$

The spreading coefficients are further given by

$$S_i = \gamma_p - \gamma_{ip} - \gamma_i \tag{2}$$

and

$$S_f = \gamma_p - \gamma_{fp} - \gamma_f \tag{3}$$

where γ denotes the surface tension or interfacial tension, and the subscript p, i, and f refer to plate, ink, and fountain solution, respectively.

Ideally, ΔS should be positive on plate image area and negative on plate non-image area. The absolute value of ΔS may be considered as a measure of stability of ink film on plate image area, or fountain solution on plate non-image area.

LITERATURE METHODS FOR MEASURING SPREADING INDEX

In literature, spreading index values have been evaluated by several methods. One method (Bassemir, 1982) was to calculate spreading coefficients from the surface tension and interfacial tension values of ink,

fountain and plates. Although surface tension values of ink and fountain solution are experimentally measurable, the surface tension of plates and interfacial tension values for ink/plate and fountain/plate interfaces are difficult, if not impossible, to measure. To overcome this difficulty, plate related surface tension and interfacial tension values are calculated using controversial theories.

In another method (Micale, 1989), contact angles of ink and fountain solution on plate surface are measured individually, and then the spreading coefficients are calculated according to the following equations:

$$S_i = \gamma_i(\cos\theta - 1) \tag{4}$$

and

$$S_f = \gamma_f(\cos\theta - 1) \tag{5}$$

where surface tensions of ink and fountain solution, γ_i and γ_f, can be measured by a conventional technique. Given spreading coefficients of ink and fountain solution, spreading index can be calculated according to the definition of spreading index (eqn. 1).

PROPOSED METHOD FOR MEASURING SPREADING INDEX

The proposed method involves rearranging eqns. 1 - 3 as follows,

$$\Delta S = f1 + f2 \tag{6}$$

where

$$f1 = (\gamma_{fp} - \gamma_{ip}) \tag{7}$$

and

$$f2 = (\gamma_f - \gamma_i). \tag{8}$$

On a plate surface covered with ink and fountain solution, f1 and f2 correspond to spreading forces on interfaces with plate and air, respectively.

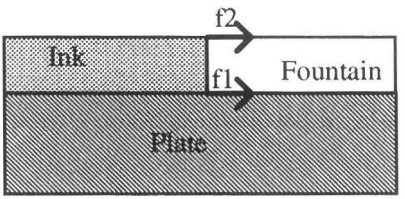

Figure 1. Spreading forces on liquid-air (f2) and liquid-plate (f1) interfaces

Of the two terms of ΔS, f2 (spreading force on the liquid-air interface) can be calculated from the surface tension values of inks and fountain solutions. Such interfacial tension values can be measured by a conventional technique such as drop weight method (Adamson, 1982). It may be noted that f2 is the same for both image area and non-image area and independent of the surface characteristics of plate.

It is f1, the spreading force at liquid-plate interface, that

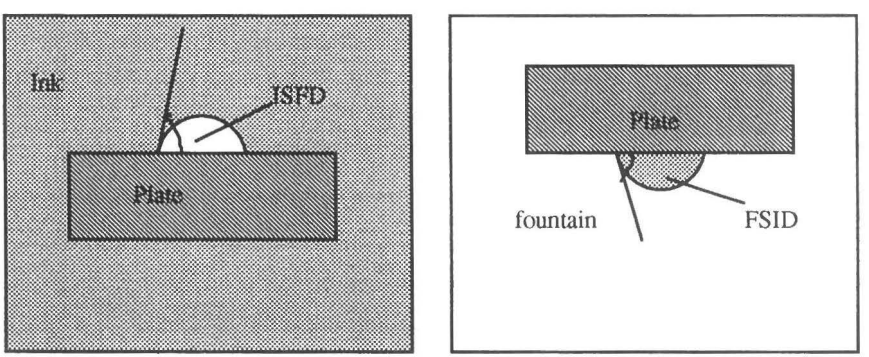

(a) (b)

Figure 2. A schematic diagram for measuring contact angles of ink-surrounded fountain droplet (ISFD), or fountain surrounded ink droplet (FSID) on a plate surface.

differentiates the plate image area and non-image area and makes

lithographic printing possible. This important property of an ink-plate-fountain system may be evaluated by measuring contact angles of ink-surrounded fountain droplet (ISFD), or fountain surrounded ink droplet (FSID) on a plate surface. The experimental setups are illustrated in Figure 2.

The above setups are applicable for the case where an ink has lower density than a fountain solution. If an ink has higher density than a fountain solution, the above experimental setups may be vertically inverted. With such experimental setups, the desired spreading force f1 on plate surface may be calculated from the measured contact angles using Young-duPre equation,

$$f1 = \gamma_{fp} - \gamma_{ip} = \gamma_{fi} \cos\theta_{FSID} \tag{9}$$

and

$$f1 = \gamma_{fp} - \gamma_{ip} = -\gamma_{fi} \cos\theta_{ISFD} \tag{10}$$

The liquid-liquid interfacial tension γ_{fi} may be determined by a conventional technique such as drop weight method.

Theoretically, the spreading force f1 determined from the two experimental setups should give the same results. Because of the opacity of inks, one would choose to measure θ_{FSID} instead of θ_{ISFD}. If desired, the latter might be calculated according to the following relationship,

$$\theta_{ISFD} = 180 - \theta_{FSID} \tag{11}$$

In reality, however, the above relationship does not always hold true because of contact angle hysteresis. Contact angle hysteresis is a phenomenon such that the contact angle of a growing droplet (advancing contact angle) is different from that of a shrinking droplet (receding contact angle). Usually, advancing contact angle is usually larger than receding angle. In most contact angle measurements by sessile drop method, the measured value usually represents an advancing contact angle. Therefore, θ_{ISFD} calculated from θ_{FSID} represent the receding contact angle of ink-surrounded fountain droplet, whereas directly measured θ_{ISFD} represents the corresponding advancing contact angle. Conversely, θ_{FSID} calculated

from θ_{ISFD} represents a receding contact angle of a fountain-surrounded ink droplet, whereas directly measured θ_{FSID} values represent the corresponding advancing contact angle.

In literature dealing with air-surrounded liquid droplets, advancing contact angles are typically used for calculating surface energy and its components (Good, 1992). In lithographic printing, however, there are two possible advancing angles, or receding contact angles, depending upon what type of droplet is concerned. In the following discussion, we will focus on the contact angle of fountain solution droplet, with θ_{ISFD} treated as advancing angle and $(180-\theta_{FSID})$ as receding angle.

INK-PLATE-FOUNTAIN MODEL SYSTEMS

In an attempt to compare different methods of evaluating spreading index and examine the ink-plate-fountain interactions, two oils were used to model inks. One is a mineral oil (Magie 470, Magie Bros.), and the other is Soy oil (technical grade, Cargill, Inc.). The model plates were prepared from five commercial negative plates, which were flood exposed and developed according to suppliers' instructions. These processed plates are coded as A-E. Two fountain solutions were used. One is pure water and the other was prepared according to the following formulation. The latter will be referred to simply as fountain solution in the following discussion.

Table 1. Formulation of a model fountain solution.

Component	wt %
Acidic fountain concentrate(Polychrome PR 637)	1.87
Alcohol substitute(Polychrome PR 628)	2.24
Isopropyl alcohol (Polychrome PR 273)	10.00
Water	85.89

RESULTS AND DISCUSSION

As seen in the previous section, calculation of spreading index values by the proposed method requires the values of γ_f, γ_i and γ_{fi}. These values were measured by drop weight method. In implementing this method, a fluid of relatively high density (d_1) was pumped out of a motorized syringe into a fluid of relatively low density (d_2). The lighter

fluid was air ($d_2 \approx 0$) when surface tension of a liquid was measured. Interfacial tension was calculated according to the following equation,

$$\gamma_{12} = \frac{980}{2\pi r f} \cdot \frac{W(d_1 - d_2)}{d_1} \tag{12}$$

where W is weight in grams per drop, r is the radius of the syringe tip, and f is a correction factor. The r values were measured from the image of a drop captured right before it detached from the syringe tip. It was noted that r varied with the wetting conditions of drop fluid on the syringe tip in the surrounding medium. The correction factor f is a function of $r/V^{1/3}$, where V is drop volume. For $r/V^{1/3} > 0.3$, f values have been tabulated (Adamson, 1982). Unfortunately, in this experiment, $r/V^{1/3}$ was in the range from 0.1 to 0.2. Therefore, the corresponding f values had to be extrapolated linearly from the available values given in the $r/V^{1/3}$ range from 0.3 to 0.6. Using this method, the calculated surface tension for water-air interface was 77 dyne/cm instead of commonly accepted value of 73 dyne/cm. To account for this error, all interfacial tension values were further corrected by a factor of 73/77.

The resulting surface tensions and interfacial tensions are listed Table 2 and Table 3, respectively.

Table 2. Surface tensions of model inks and fountain solutions.

liquid	d (g/cm^3)	γ (dyne/cm)
Soy oil	0.91	41
Mineral oil	0.79	30
water	1.00	73
Fountain solution	0.99	33

Table 3. Interfacial tensions at the interfaces of model inks and model fountain solutions.

	water (dyne/cm)	Fountain (dyne/cm)
Soy oil	16	13
Mineral oil	19	14

The contact angles of ink-surrounded fountain droplets and fountain surrounded ink droplets were measured using the experimental setups illustrated in Figure 2. The measurements were carried out on a

video contact angle apparatus (VCA 2000, Advanced Surface Technology). This apparatus allows us to capture droplet shapes at a speed of six frames per second. Although not sufficient for monitoring the process of reaching a mechanical equilibrium at a three-phase contact line, this image caption speed is enough to monitor relatively slow processes such as contact angle changes as a result of surface adsorption and structural re-orientation at a solid surface. Figure 3 shows the contact angle variation of a fountain droplet surrounded by Soy oil on five model plates after the initial contact.

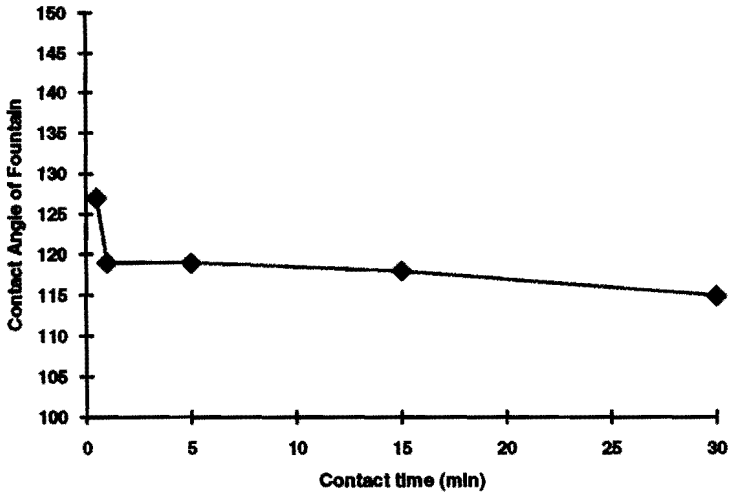

Figure 3. Contact angle variation of a fountain droplet surrounded by Soy oil on plate A after the initial contact.

It can be seen that the contact angle reached a plateau in one minute after the initial contact. Figure 4 (ISFD) shows the drop shape captured at that moment.

Figure 4 also shows the drop shape of an ink droplet surrounded by a fountain solution captured one minute after initial contact. It may be noted from Figure 4 that contact angles of both FSID and ISFD are larger than 90°. Although the large contact angle of ISFD on the plate image area may be considered as normal, the large contact angle of FSID on the plate image area is not what we would expect. However, such results were

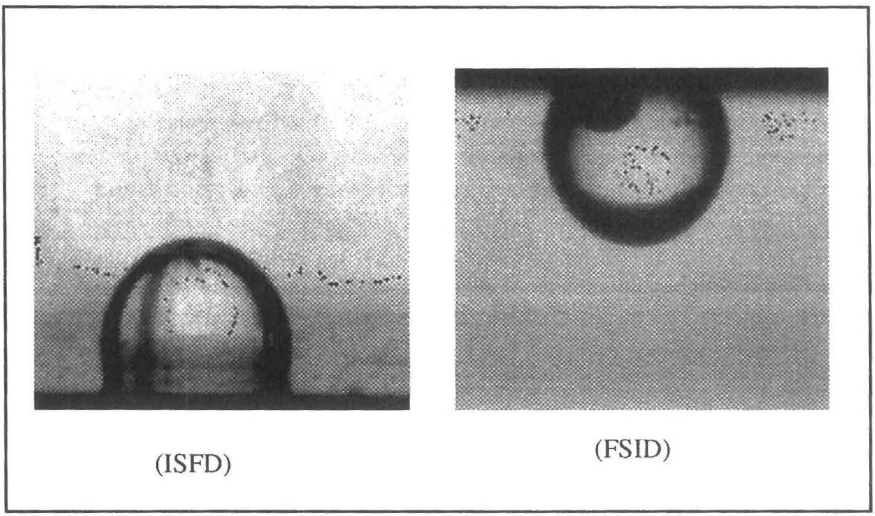

Figure 4. Shapes of a fountain droplet surrounded by Soy oil (ISFD) and an ink droplet surrounded by fountain solution (FSID) on the image area of plate A.

rather typical in our model systems. These results are listed in the following tables.

Table 4. Contact angle of fountain droplet on plate image area (deg).

Plate	In Soy oil		In Magie oil	
(Image area)	θ_{ISFD}	$180-\theta_{FSID}$	θ_{ISFD}	$180-\theta_{FSID}$
A	119	65	97	72
B	111	74	98	62
C	141	76	136	64
D	120	59	114	51
E	108	67	113	60

Table 5. Contact angles of water droplet on plate image area (deg.)

Plate	In Soy oil		In Magie oil	
(Image area)	θ_{ISFD}	$180-\theta_{FSID}$	θ_{ISFD}	$180-\theta_{FSID}$
A	124	64	101	69
B	110	58	101	64
C	142	55	128	62
D	145	52	158	55
E	124	54	155	63

As mentioned earlier, when θ_{ISFD} is considered as an advancing angle of fountain solutions, $(180-\theta_{FSID})$ represents the corresponding receding angle. The data in the above two tables indicate strong hysteresis. Such hysteresis may be attributed to the interactions among ink, fountain and plate. For example, interaction between fountain solution and plate may result in restructuring of plate surface such that the plate surface is more compatible with fountain. As a consequence, advancing of ink into fountain solution becomes more difficult. Similar interactions may exist between plate and ink. Such interactions will render the plate surface more fountain repellent.

Given the contact angles of FSID and ISFD, and related liquid-air and liquid-liquid interfacial tensions, we now can calculate the spreading index values. The results are listed in the following tables.

Table 6. Spreading index values calculated from the contact angles of ISFD (dyne/cm).

Plate	Water		Fountain	
(Image area)	Soy oil	Magie oil	Soy oil	Magie Oil
A	39	46	-1.8	5.2
B	36	46	-3.5	5.4
C	41	51	1.9	13
D	42	56	-1.7	9.1
E	39	55	-4.1	8.9

Table 7. Spreading index values calculated from the contact angles of FSID (dyne/cm).

Plate	Water		Fountain	
(Image area)	Soy oil	Magie oil	Soy oil	Magie Oil
A	26	38	-13	-0.73
B	25	37	-12	-2.9
C	24	36	-11	-2.5
D	24	35	-15	-5.1
E	24	37	-13	-3.4

As noted from the above tables, ink-plate-fountain systems with Magie oil have larger spreading index values than the corresponding systems with Soy oil, indicating that Magie oil has stronger affinity with plate image area than Soy oil. It can also be seen that using fountain solution in place of pure water reduces the affinity between ink and plate image area. This phenomenon may be attributed to the fact that the surface active species in fountain solution drastically reduce surface tension and enhance the spreading power of fountain solution relative to the spreading power of ink. Such enhancement may occur both at liquid-air interface (f2) and at liquid-plate interface (f1). The effect on f2 can also be seen from the data in Table 2, which show that the surface tension of fountain solution is much lower than water, even lower than Soy oil. Therefore, in the Soy oil-fountain-plate systems, f2 is negative and offsets small positive values of f1 calculated from ISFD. The data from Soy oil droplets surrounded by fountain solution even give negative values of f1, for such contact angles (given in Table 4 in terms of $180-\theta_{FSID}$) were larger than 90.

At this point, one may ask whether the spreading index data on soy oil-plate-fountain solution would predict a free spreading of fountain solution. To answer this question, let us consider an imaginary state shown in Figure1. Since f2 is negative, the air-ink-fountain contact line tends to advance toward the ink. Whether the plate-ink-fountain contact line will follow is determined by the f1 value for the case of fountain advancing toward ink, namely, the f1 value calculated from the contact angle of ISFD. The positive value of f1 indicates a resistance against the spreading of fountain solution. Because of this resistance, the ink-fountain interface will be stretched, which is resisted by the interfacial tension γ_{fi}. Such resistance force plus other boundary constraints for a system with a given ink-water ratio may stop the spreading of fountain solution. Furthermore, in real soy oil based inks, presence of other components may also ease up the

unfavorable spreading index. These components may reduce the surface tension of inks so that f2 and thus ΔS become positive.

Table 8. Contact angles of air surrounded liquid droplets (deg.)

Plate	Soy oil	Magie oil	Fountain	Water
A	15	0	42	64
B	15	0	45	64
C	25	0	46	90
D	37	18	43	95
E	31	13	44	81

Spreading index can also be calculated from the contact angles of ink and fountain solution droplets surrounded by air. For comparison, such contact angles of model inks and fountain solutions were measured using our video contact angle system. It was noted that the contact angle variation with time was faster for air-surrounded droplets. Such variation may be attributed to surface evaporation. Because of this phenomenon, contact angles were calculated from images captured within five seconds after initial contact. The results are listed below.

Given the contact angles of air surrounded liquid droplets in Table 8, and the liquid surface tension values given in Table 2, the spreading index values can be calculated using eqns. 1, 4, and 5. The results are listed in the following table.

Spreading index values calculated from the contact angles of air surrounded liquid droplets (dyne/cm).

Plate	Water		Fountain	
(Image area)	Soy oil	Magie oil	Soy oil	Magie Oil
A	39	(41+)[a]	7.2	8.6
B	39	(41+)[a]	8.4	9.8
C	69	73	6.3	10
D	71	78	0.64	7.5
E	55	61	3.5	8.6

[a] cannot be determined by this method because of zero contact angle.

In comparison with the ISFD data given in Table 6, the spreading index values calculated from air surrounded liquid droplets are larger,

especially for plates D and E with oil-water systems, and for all plates with Soy oil-fountain systems. Such differences may be attributed to three-phase interactions such as inter-diffusion and surface adsorptions. Apparently, the data calculated from contact angles of air surrounded droplets do not reflect such interactions.

CONCLUSIONS

A method has been proposed to measure the spreading index of an ink-plate-fountain system from the contact angles of ink-surrounded fountain droplets and fountain surrounded ink droplets. In comparison to previous method of using the contact angles of air-surrounded liquid droplets, the proposed method exhibits the following features:

1. Individual measurement of competitive spreading on liquid-air and liquid-plate interfaces.

2. Capability of probing three phase interactions

3. Capability of studying hysteresis in competitive spreading of ink and fountain

4. Applicability to systems with zero contact angle in air.

Application of the proposed method to model ink-plate-fountain systems has shown that alcohols and other components in fountain solution have unfavorable effects on the spreading index values in the image area as compared with pure water. Of cause, alcohols and other components are used for the purpose of improving other properties of a lithographic printing system, especially the performance in the non-image area. Application of the proposed method to plate non-image area will be a subject for future study.

It has also been shown that Magie oil has higher spreading index than soy oil. Such difference is mainly caused by the surface tension difference between the two oils.

The differences among several plates are evident. A more systematic study will be carried out in the future.

LITERATURE CITED

Adamson, A. W.

1982. "Physical Chemistry of Surfaces" (John Wiley & Sons, New York) 4th ed., pp20-23.

Bassemir, R. W.; and Shubert, F.

1982. "Relationship of Surface Energy of Lithographic Plates and Inks to Printability", TAGA Proceedings (Technical Association of the Graphic Arts, Rochester) pp290-310.

Good, R. J.

1992. "Contact angle, wetting, and adhesion: a critical review", J. Adhesion Sci. Technol. Vol.6, No. 12, pp1269-1302.

MacPhee, J.

1979. "An Engineer's Analysis of the Lithographic Printing Process", TAGA Proceedings (Technical Association of the Graphic Arts, Rochester) pp237-277.

Micale, F. J.; Iwasa, S.; Lavelle, J.; Sunday, S.; and Fetsko, J. M.

1989. "The Role of Wetting, Part I. Lithography", American Ink Maker September, pp 44-54.

1989. "The Role of Wetting in Printing", TAGA Proceedings (Technical Association of the Graphic Arts, Rochester), pp 309-329.